

# Experimental apparatus for detection of radiative decay of $^{229}\text{Th}$ isomer from Th-doped $\text{CaF}_2$

Takahiro Hiraki on behalf of the collaboration<sup>1\*</sup>

<sup>1\*</sup>Research Institute for Interdisciplinary Science, Okayama University,  
1-1-1 Tsushima-naka, Kita-ku, Okayama, 7008530, Japan.

Corresponding author(s). E-mail(s): [thiraki@okayama-u.ac.jp](mailto:thiraki@okayama-u.ac.jp) ;

## Abstract

Among all the nuclei, Thorium-229 has the lowest excited level at approximately 8.3 eV. This level is an isomeric state with a long radiative lifetime. Therefore,  $^{229}\text{Th}$  can be excited to the isomeric state using a vacuum ultraviolet laser and is expected to have applications such as in frequency standards. Our group has been conducting experiments to excite  $^{229}\text{Th}$  to the isomeric state via the second excited state using the high-intensity X-ray beam available at the SPring-8 facility. To detect vacuum ultraviolet photons from the isomeric state of  $^{229}\text{Th}$ , a dedicated apparatus was constructed. We employed  $^{229}\text{Th}$ -doped  $\text{CaF}_2$  crystals as the irradiation target. Because these targets emit numerous scintillation photons due to nuclear decay and X-ray beam irradiation, detectors are required to significantly reduce these background events. To achieve this, we adopted dichroic mirrors and a photomultiplier tube for detecting scintillation photons by nuclear decay, in addition to a solar-blind photomultiplier tube for detecting decay photons from the isomeric state of  $^{229}\text{Th}$ . In this proceedings paper, we describe the experimental apparatus used in the beamtime in 2023.

**Keywords:**  $^{229}\text{Th}$ , isomeric state, vacuum ultraviolet light, X-ray beam, SPring-8, detector

## 1 Introduction

The excitation energy of the first excited state of the nucleus of  $^{229}\text{Th}$  ( $^{229\text{m}}\text{Th}$ ) is about 8 electron volts (eV), the smallest and uniquely low among all known nuclei. This energy corresponds to a wavelength of approximately 150 nm, a wavelength range that can be accessed using today's advanced laser spectroscopy technology. Therefore,

it is possible to create an atomic clock, using the transition between the ground state and the first excited state of  $^{229}\text{Th}$  [1–3]. Unlike atomic clocks, which are realized using optical lattices or ion traps, it is considered possible to construct solid-state nuclear clocks [4, 5]. Since the proposal of a nuclear clock [1], various applications of nuclear clocks have been proposed [6, 7].

In recent years, research on  $^{229}\text{Th}$  has made great progress [8–15], and several review articles have been published [6, 7, 16, 17]. Neutral atomic  $^{229\text{m}}\text{Th}$  has undergone internal conversion (IC) and its half-life was measured to be  $7(1) \mu\text{s}$  [9]. If  $^{229}\text{Th}$  is doped in a crystal with a large band gap, IC can be avoided. Recently, the first observation of radiative decay of  $^{229\text{m}}\text{Th}$  was reported [13]. In [13],  $^{229}\text{Fr}$  and  $^{229}\text{Ra}$  ion beam produced at the ISOLDE facility at CERN was implanted near the surfaces of  $\text{MgF}_2$  and  $\text{CaF}_2$  crystals. The measured wavelength of radiative decay photons was  $\lambda_{\text{isomer}} = 148.71(41) \text{ nm}$ , which corresponds to a photon energy of  $E_{\text{isomer}} = 8.338(24) \text{ eV}$ . The measured half-life of  $^{229\text{m}}\text{Th}$  embedded near the surface of  $\text{MgF}_2$  is  $670(102) \text{ s}$ . Note that the magnetic dipole transition rate in dielectric media with refractive index  $n$  is  $n^3$  times higher than that in vacuum [18]. The conversion of the half-life of  $^{229\text{m}}\text{Th}$  in a vacuum from the reported value needs to be carefully considered. This is because the implantation depth of the ion beam is shorter than  $\lambda_{\text{isomer}}$  [13] and it is not clear whether the refractive index effect should be treated as it is.

Direct excitation from the ground state to the first excited state of  $^{229}\text{Th}$  has not yet been realized [19–21]; however, our group succeeded in producing  $^{229\text{m}}\text{Th}$  from the ground state indirectly [14]. An X-ray beam available at synchrotron radiation facilities is used to excite the ground state of  $^{229}\text{Th}$  nuclei to the second excited state, where roughly half of them are deexcited to  $^{229\text{m}}\text{Th}$ .

After the success of indirect excitation, we started to construct a setup for the detection of the radiative decay photons from  $^{229\text{m}}\text{Th}$ . Regarding the target for detecting vacuum ultraviolet (VUV) photons from  $^{229\text{m}}\text{Th}$ , we employed  $\text{CaF}_2$  crystals doped with  $^{229}\text{Th}$ , where crystal properties were well studied and a high  $^{229}\text{Th}$  doping concentration was achieved [22, 23]. Using these crystals, a half-life measurement of  $^{229\text{m}}\text{Th}$  inside  $\text{CaF}_2$  and conversion to half-life in a vacuum are possible without having to be concerned about the refractive index effect. In this proceedings paper, details of the experimental apparatus are described.

## 2 Experimental setup

### 2.1 SPring-8

The experiment was conducted at the BL19LXU beamline of the SPring-8 facility. In this beamline, a high-brilliance X-ray beam is available thanks to the 27-meter-long undulator. The X-ray beam energy was selected using monochromator sets. One of the reasons for this is to reduce the crystal transmittance by beam irradiation. We used one Si(111), one Si(660), and one Si(880) monochromator set<sup>1</sup> for extracting the 29.2 keV X-ray beam, which corresponds to the second excitation energy of  $^{229}\text{Th}$  nuclei. Throughout the experiment, ionization chambers continuously recorded the

---

<sup>1</sup>The Si(880) monochromator was installed in beamtime of 2023. This is found to be important for avoiding damage to the crystal target.

X-ray flux per second. Beam profile and absolute beam intensity measurements were occasionally performed using a silicon PIN detector. The typical intensity of the X-ray beam downstream of the Si(880) monochromator was  $1-2 \times 10^{11}$  /s<sup>2</sup>. The absolute X-ray energy monitor [24] was located in the downstream-most area of the experimental hutch. It takes a few minutes to obtain one absolute X-ray energy value. The energy of the X-ray beam can be adjusted by mainly changing the reflection angle of the Si(660) or Si(880) monochromator set.

## 2.2 Detection setup of vacuum ultraviolet light from <sup>229m</sup>Th

In this experiment, there exist mainly two types of background events. The first is photoluminescence (also called X-ray excited optical luminescence). When an X-ray beam is injected into the crystal target, scintillation photons with various wavelengths are emitted. After beam irradiation stops, the photoluminescence intensity gradually decreases. The second is radioluminescence, which results from scintillation caused by decays of <sup>229</sup>Th and daughter nuclei. In some cases of  $\beta$ -decay (the kinetic energy of the decay electron is higher than roughly 150 keV), Cerenkov photons are also emitted. The event rates of the background are several orders of magnitude higher than the production rate of <sup>229m</sup>Th in this experimental condition. Therefore, although background cancellation can be performed using a comparison of data between the on-resonance and off-resonance conditions of the incident X-ray beam energy, strong background rejection in the detection system is still essential.

Figure 1 shows an overview of the vacuum chamber used in this experiment. This chamber was placed on a surface plate on a motorized workbench for alignment between the target and the X-ray beam. At the beam injection parts of the chamber, beryllium foils were used to reduce the X-ray beam loss. When the X-ray beam was irradiated to the target crystal, intense scattering and scintillation lights were emitted from the crystal. To avoid damage to the detector by the injection of strong light, the point of the X-ray beam irradiation was separated. After beam irradiation, the target holder was moved using the pneumatic stage. The movement time was approximately one second.

---

<sup>2</sup>The typical X-ray beam intensity between the Si(660) and Si(880) monochromator is  $9.5 \times 10^{11}$  /s.

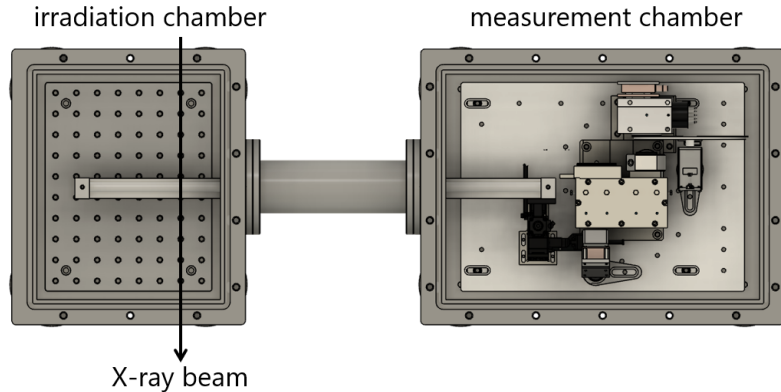


**Fig. 1** Experimental setup for the detection of the VUV signal from  $^{229\text{m}}\text{Th}$ . The X-ray beam passed through the left chamber, and light from the crystal target was measured in the right chamber.

In this experiment, several  $^{229}\text{Th}$ -doped  $\text{CaF}_2$  targets were used.  $^{229}\text{Th}$ -doped  $\text{CaF}_2$  crystals were produced by TU Wien. For this experiment, small crystals of about  $1\text{ mm}^3$  are suitable because the X-ray beam diameter is roughly  $1\text{ mm}$  and the attenuation length of the  $29.2\text{ keV}$  X-ray beam inside  $\text{CaF}_2$  is approximately  $1.3\text{ mm}^3$ . Some crystal ingots produced were cut into several crystals, and we used roughly  $1\text{ mm}^3$  crystals with a density of up to roughly  $5 \times 10^{15} / \text{mm}^3$ .

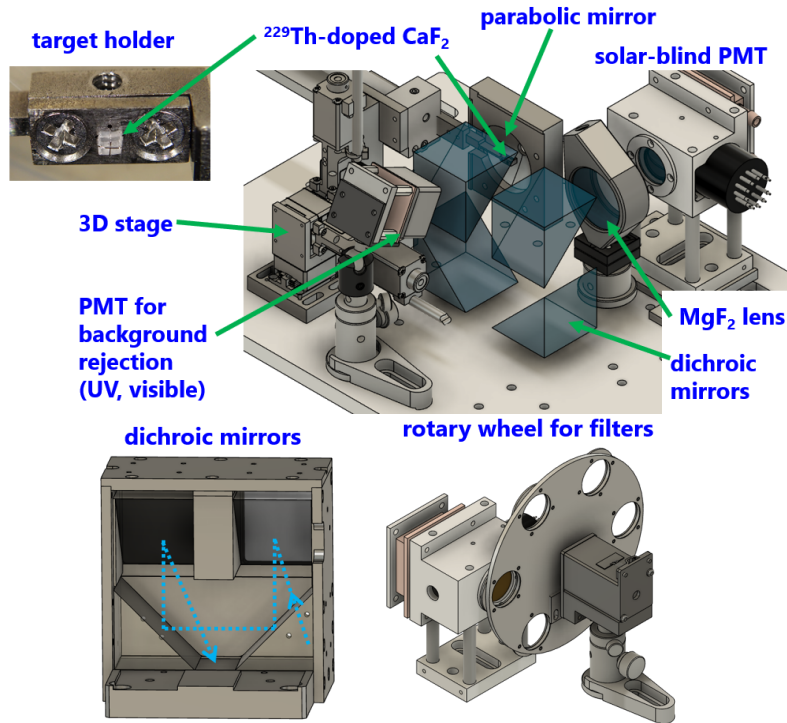
Figure 2 (top left) shows a photograph of the target holder. The target was fixed using SUS wires ( $50\ \mu\text{m}\varnothing$ ) to the SUS holder. As the crystal target is irradiated by the X-ray beam, the transmittance of the crystal decreases. For the recovery of transmittance, each irradiated crystal was sometimes replaced during beamtime, and annealed. The damaged crystal was heated to approximately  $400^\circ\text{C}$  by the jacket heater inside the vacuum nipple for one hour as part of the annealing procedure. The temperature change between room temperature and  $400^\circ\text{C}$  is slow to avoid crystal damage, and it took about 10 hours in total to complete one annealing process. When a crystal was replaced from one to another, the used crystal was annealed before the next use. The duration of one beamtime was about one week and within that period, the crystals were annealed a few times in total.

Figure 2 (top right) shows the schematic view of the setup for detecting vacuum ultraviolet (VUV) light from  $^{229\text{m}}\text{Th}$ . After beam irradiation, the target was moved and then placed in front of the custom-made parabolic mirror (OptoSigma,  $40\text{ mm}\varnothing$ ). For the alignment between the target and the parabolic mirror, three-dimensional stages (OptoSigma) were used, where optimization was performed so that the radioluminescence event rate was the highest. To reduce background events, we prepared dichroic mirrors (custom-made coating by OptoSigma). Right-angle prisms were selected for the host material (Thorlabs, PS612) so that background by reflection from the rear surface was reduced. The reflectance of a dichroic mirror at the peak wavelength is higher than 80%, which is much higher than the transmittance of

<sup>3</sup>In terms of the reduction of the radioluminescence background events, a smaller crystal is better.

commercial band-pass filters in the VUV region. Before signal photons hit the detector, they reflect in both horizontal and vertical directions, as shown in Fig. 2 (bottom left). The overall reflectance after four reflections is lower than that of the four consecutive horizontal reflections because the reflectance of the *s*-polarized light of each dichroic mirror is higher than that of the *p*-polarized light. Thus, these dichroic mirrors efficiently reduce the background photons regardless of their polarization direction.

A custom-made uncoated MgF<sub>2</sub> lens (Pier Optics, 40 mm $\varnothing$ ) was placed downstream of the dichroic mirrors to focus the light from the dichroic mirrors. A solar-blind photomultiplier tube (PMT, Hamamatsu, R10454) was used to detect the VUV signal. To reduce dark-photon background events, the VUV PMT was installed in the metal holder, which was cooled to -30°C by using a Peltier temperature controller. The event rate of the dark-photon background is less than 0.1 cps. Band-pass filters (purchased from Teledyne Acton Optics and Pelham Research Optical LLC, 1 inch $\varnothing$ ) mounted to the rotary holder could be inserted in front of the solar-blind PMT during measurement, as shown in Fig. 2 (bottom right). These filters were used for measuring  $\lambda_{\text{isomer}}$ .



**Fig. 2** Schematic view of the VUV detector.

Another PMT (Hamamatsu, R11265-203) was placed downstream of the first dichroic mirror to reduce radioluminescence background events. This PMT detects ultraviolet and visible photons produced by the scintillation of the target crystal.

## 2.3 Data acquisition

Figure 3 shows the scheme of data acquisition. Waveforms of the two PMTs were amplified and recorded using an oscilloscope (National Instruments, PXIe-5162). Raw waveform data were saved on a PC with an SSD connected to the oscilloscope via a LAN cable. The data acquisition rate is at most several hundred Hz, where most of the events are radioluminescence. During measurement, clock pulse signals were prepared using a pulse generator (Stanford Research Systems, DG535). The channels of the solar-blind PMT and the clock pulse were combined and recorded as the trigger channel to estimate the data acquisition and background rejection efficiencies.

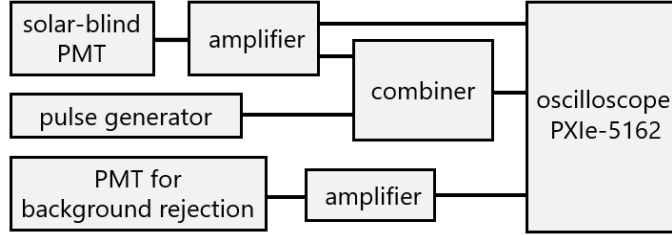


**Fig. 3** Schematic view of data acquisition. The combined channel of the solar-blind PMT and the pulse generator was used as the trigger channel.

## 3 Performance of the experimental setup for detecting VUV photons

### 3.1 Waveform information

Figure 4 shows examples of waveforms. At the beginning of each measurement, strong photoluminescence was observed. This causes a drift of the ground level of the PMT for background rejection. Photoluminescence has multiple lifetime components and its amount decreases over time from the beginning of a measurement [25]. When  $\alpha$ - or  $\beta$ -decay of  $^{229}\text{Th}$  or daughter nuclei occurred, numerous scintillation photons (radioluminescence) were emitted from the target crystal. In the case of  $\beta$ -decay, deposited energy in a crystal is sometimes low and the corresponding peak height of radioluminescence is small.

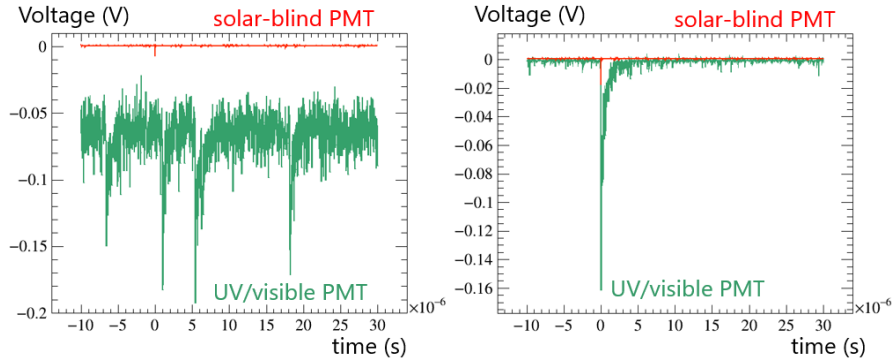


**Fig. 4** Examples of waveforms. Left: example near the beginning of the measurement. Right: example of when near the end of the measurement. Here, events triggered by the solar-blind PMT are chosen. Trigger timing is set to the origin of time.

### 3.2 Rejection of the radioluminescence background

Figure 5 shows an example of the time spectra of observed events triggered by the solar-blind PMT. These data were obtained under the off-resonance energy condition of the X-ray beam. Before background rejection, most of the triggered events consisted of radioluminescence. These radioluminescence events were mostly rejected using waveform information. If there is a radioluminescence peak near the timing when the VUV PMT detected a photon, this event is rejected. If only timing information is used, many radioluminescence background events remain. This is because this rejection fails mainly when multiple radioluminescence waveforms overlap. Thus, pulse height information near the timing is also used for background rejection. The rejection conditions of the radioluminescence background depend on the experimental conditions. For instance, the threshold value of the peak pulse height of radioluminescence depends on the elapsed time from the start of the measurement because the strength of photoluminescence decreases during measurement. Note that it is difficult to completely reject the radioluminescence background because in some cases of  $\beta$ -decay, the number of emitted scintillation photons is quite low. After background rejection, most radioluminescence events were successfully rejected. The remaining events were mainly photoluminescence background, where the rate of these events depended on the elapsed time from the start of measurement (the end of the irradiation of the X-ray beam). The data acquisition efficiency and the event selection efficiency, i.e., the ratio of the remaining  $^{229}\text{Th}$  radiative decay signal after background rejection using the waveform information of the UV/visible PMT, depend on the activity of the crystal used. In the case where the  $^{229}\text{Th}$  density is approximately  $4 \times 10^{15} / \text{mm}^3$ , the data acquisition efficiency is 98–99% and the event selection efficiency is roughly 30% in this experimental setup and analyses. Although the condition of background rejection depends on the elapsed time from the start of measurement, this can be selected appropriately to keep the event selection efficiency almost constant.

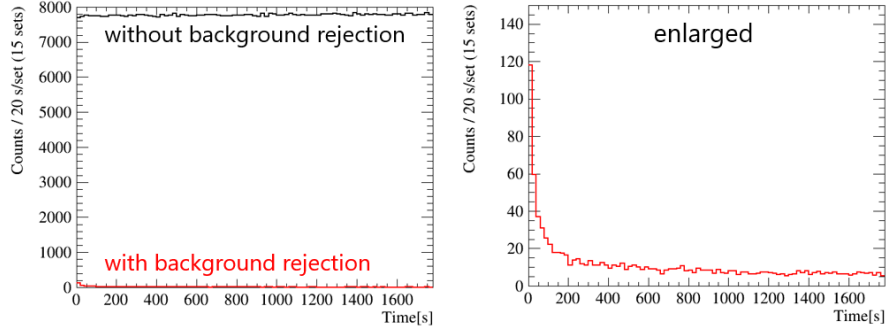


**Fig. 5** Time spectra of observed events triggered by the solar-blind PMT. These data were obtained under the off-resonance energy condition of the X-ray beam. The right plot is an enlarged view of the left plot.

## 4 Conclusion

To measure the radiative decay signal from  $^{229\text{m}}\text{Th}$  which is doped inside crystals, we performed experiments at SPring-8, a synchrotron radiation facility located in Japan. We produce  $^{229\text{m}}\text{Th}$  through the second excited state using a monochromatized 29.2 keV X-ray beam. To observe a clear signal, it is important to use three sets of silicon monochromators in the beamline, crystals with a high  $^{229}\text{Th}$  density, and an apparatus with efficient signal detection and strong background rejection. For the reduction of luminescence background photons from  $^{229}\text{Th}$ -doped  $\text{CaF}_2$  crystal target, we constructed a setup where dichroic mirrors and two types of PMT were used. The radioluminescence background can be mostly ignored by using waveform information of the UV/visible PMT, and the photoluminescence background can be subtracted by taking both on-resonance and off-resonance data. This measurement system we have developed can be used as is for experiments of direct laser excitation of  $^{229}\text{Th}$  doped in a crystal target.

**Acknowledgments.** The synchrotron radiation experiments were performed at the BL19LXU line of SPring-8 with the approval of the Japan Synchrotron Radiation Research Institute (JASRI) and RIKEN.

## Declarations

- Funding  
This work was supported by JSPS KAKENHI Grant Numbers JP19K14740 and JP21H01094 and Itoh Science Foundation for a grant.
- Conflict of interest/Competing interests (check journal-specific guidelines for which heading to use)  
The authors declare no competing interests.
- Ethics approval  
not applicable
- Availability of data and materials

Requests should be addressed to the corresponding author.

## Appendix A Measurement of optical components

For the estimation of the expected number of detected signal photons from  $^{229\text{m}}\text{Th}$  or  $\lambda_{\text{isomer}}$ , we measured the transmittance or reflectance data of optical components, such as dichroic mirrors and VUV band-pass filters. Figure A1 shows a schematic view of the optical property measurement system. The monochromatic VUV light beam is generated using the deuterium lamp (Heraeus, D200VUV) and the spectrometer (Shinku-kogaku, VMK-200-II). Each sample is placed on motorized stages so that position and angle dependence can be measured. The PMT (Hamamatsu, R6836) is also mounted on another motorized rotation stage so that both transmittance and reflectance can be measured.

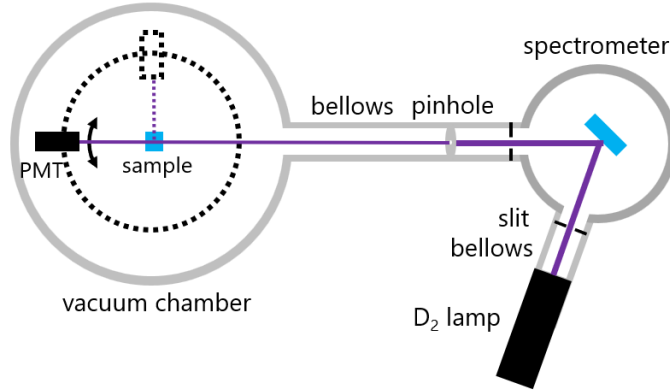


Fig. A1 Schematic view of the optical property measurement system.

## References

- [1] Peik, E. and Tamm, C.: Nuclear laser spectroscopy of the 3.5 eV transition in Th-229. *Euro. Phys. Lett.* **61**, 181 (2003). <https://dx.doi.org/10.1209/epl/i2003-00210-x>
- [2] Campbell, C.J., Radnaev, A.G., Kuzmich, A., Dzuba, V.A., Flambaum, V.V., and Derevianko, A.: Single-Ion Nuclear Clock for Metrology at the 19th Decimal Place. *Phys. Rev. Lett.* **108**, 120802 (2012). <https://doi.org/10.1103/PhysRevLett.108.120802>
- [3] Peik, E. and Okhapkin, M: Nuclear clocks based on resonant excitation of  $\gamma$ -transitions. *C. R. Physique* **16**, 516-523 (2015). <https://doi.org/10.1016/j.crhy.2015.02.007>
- [4] Rellergert, W.G., DeMille, D., Greco, R.R., Hehlen, M.P., Torgerson, J.R. and Hudson, E.R.: Constraining the Evolution of the Fundamental Constants with a

Solid-State Optical Frequency Reference Based on the  $^{229}\text{Th}$  Nucleus. *Phys. Rev. Lett.* **104**, 200802 (2010). <https://doi.org/10.1103/PhysRevLett.104.200802>

- [5] Kazakov, G.A., Litvinov, A.N., Romanenko, V.I., Yatsenko, L.P., Romanenko, A.V. , Schreitl, M, Winkler, G., and Schumm, T.: Performance of a  $^{229}\text{Th}$  Thorium solid-state nuclear clock. *New J. Phys.* **14**, 083019 (2012). <https://doi.org/10.1088/1367-2630/14/8/083019>
- [6] von der Wense, L. and Seiferle, B.: The  $^{229}\text{Th}$  isomer: prospects for a nuclear optical clock. *Eur. Phys. J. A* **56**, 277 (2020). <https://doi.org/10.1140/epja/s10050-020-00263-0>
- [7] Peik, E., Schumm, T., Safronova, M.S., Pálffy, A., Weitenberg, J., and Thirolf, P.G.: Nuclear clocks for testing fundamental physics. *Quantum Sci. Technol.* **6**, 034002 (2021). <https://doi.org/10.1088/2058-9565/abe9c2>
- [8] von der Wense, L. *et al.*: Direct detection of the  $^{229}\text{Th}$  nuclear clock transition. *Nature* **533**, 47-51 (2016). <https://doi.org/10.1038/nature17669>
- [9] Seiferle, B. von der Wense, L., and Thirolf, P.G.: Lifetime Measurement of the  $^{229}\text{Th}$  Nuclear Isomer. *Phys. Rev. Lett.* **118**, 042501 (2017). <https://doi.org/10.1103/PhysRevLett.118.042501>
- [10] Thielking, J. *et al.*: Laser spectroscopic characterization of the nuclear-clock isomer  $^{229\text{m}}\text{Th}$ . *Nature* **556**, 321-325 (2018). <https://doi.org/10.1038/s41586-018-0011-8>
- [11] Seiferle, B. *et al.*: Energy of the  $^{229}\text{Th}$  nuclear clock transition. *Nature* **573**, 243-246 (2019). <https://doi.org/10.1038/s41586-019-1533-4>
- [12] Sikorsky, T. *et al.*: Measurement of the  $^{229}\text{Th}$  Isomer Energy with a Magnetic Microcalorimeter. *Phys. Rev. Lett.* **125**, 142503 (2020). <https://doi.org/10.1103/PhysRevLett.125.142503>
- [13] Kraemer, S. *et al.*: Observation of the radiative decay of the  $^{229}\text{Th}$  nuclear clock isomer. *Nature* **617**, 706-710 (2023). <https://doi.org/10.1038/s41586-023-05894-z>
- [14] Masuda, T. *et al.*: X-ray pumping of the  $^{229}\text{Th}$  nuclear clock isomer. *Nature* **573**, 238-242 (2019). <https://doi.org/10.1038/s41586-019-1542-3>
- [15] Shigekawa, Y. *et al.*: Estimation of radiative half-life of  $^{229\text{m}}\text{Th}$  by half-life measurement of other nuclear excited states in  $^{229}\text{Th}$ . *Phys. Rev. C* **104**, 024306 (2021). <https://doi.org/10.1103/PhysRevC.104.024306>
- [16] Thirolf, P.G., Seiferle, B., and von der Wense, L.: The  $^{229}\text{Th}$ -thorium isomer: doorway to the road from the atomic clock to the nuclear clock. *J. Phys. B: At.*

- Mol. Opt. Phys. **52**, 203001 (2019). <https://doi.org/10.1088/1361-6455/ab29b8>
- [17] Beeks, K., Sikorsky, T., Schumm, T., Thielking, J., Okhapkin, M.V., and Peik, E.: The thorium-229 low-energy isomer and the nuclear clock. Nat. Rev. Phys. **3**, 238-248 (2021). <https://doi.org/10.1038/s42254-021-00286-6>
- [18] Tkalya, E.V.: Spontaneous emission probability for M1 transition in a dielectric medium:  $^{229\text{m}}\text{Th}$  ( $3/2^+$ ,  $3.5\pm 1.0$  eV) decay. JETP Lett. **71**, 311-313 (2000). <https://doi.org/10.1134/1.568349>
- [19] Jeet, J., Schneider, C., Sullivan, S.T., Rellergert, W.G., Mirzadeh, S., Casanholo, A., Jenssen, H.P., Tkalya, E.V., and Hudson, E.R.: Results of a Direct Search Using Synchrotron Radiation for the Low-Energy  $^{229}\text{Th}$  Nuclear Isomeric Transition. Phys. Rev. Lett. **114**, 253001 (2015). <https://doi.org/10.1103/PhysRevLett.114.253001>
- [20] Yamaguchi, A., Kolbe, M., Kaser, H., Reichel, T., Gottwald, A., and Peik, E.: Experimental search for the low-energy nuclear transition in  $^{229}\text{Th}$  with undulator radiation. New J. Phys. **17**, 053053 (2015). <https://doi.org/10.1088/1367-2630/17/5/053053>
- [21] Stellmer, S., Kazakov, G., Schreitl, M., Kaser, H., Kolbe, M., and Schumm, T.: Attempt to optically excite the nuclear isomer in  $^{229}\text{Th}$ . Phys. Rev. A **97**, 062506 (2018). <https://doi.org/10.1103/PhysRevA.97.062506>
- [22] Dessovic, P., Mohn, P., Jackson, R.A., Winkler, G., Schreitl, M., Kazakov, G., and Schumm, T.:  $^{229}\text{Th}$  Thorium-doped calcium fluoride for nuclear laser spectroscopy. J. Phys.: Condens. Matter **26**, 105402 (2014). <https://doi.org/10.1088/0953-8984/26/10/105402>
- [23] Beeks, K. *et al.*: Growth and characterization of thorium-doped calcium fluoride single crystals. Sci. Rep. **13**, 3897 (2023). <https://doi.org/10.1038/s41598-023-31045-5>
- [24] Masuda, T. *et al.*: Absolute X-ray energy measurement using a high-accuracy angle encoder. J. Synchrotron Radiat., **28**, 111-119 (2021). <https://doi.org/10.1107/S1600577520014526>
- [25] Stellmer, S., Schreitl, M., and Schumm, T.: Radioluminescence and photoluminescence of Th:CaF<sub>2</sub> crystals. Sci. Rep. **5**, 15580 (2015). <https://doi.org/10.1038/srep15580>